energies

MDPI

Article

Viscosity Models for Polymer Free CO_2 Foam Fracturing Fluid with the Effect of Surfactant Concentration, Salinity and Shear Rate

Shehzad Ahmed [1,*], Khaled Abdalla Elraies [1], Muhammad Rehan Hashmet [2] and Alvinda Sri Hanamertani [1]

[1] Department of Petroleum Engineering, Universiti Teknologi PETRONAS, Seri Iskandar 32610, Perak, Malaysia; Khaled.elraies@utp.edu.my (K.A.E.); alvindamertani12@gmail.com (A.S.H.)

[2] Department of Petroleum Engineering, Petroleum Institute, Khalifa University of Science and Technology, P.O. Box 2533, Abu Dhabi, United Arab Emirates; mhashmet@pi.ac.ae

* Correspondence: shehzadahmed904@yahoo.com; Tel.: +60-5-368-7037

Received: 13 October 2017; Accepted: 17 November 2017; Published: 26 November 2017

Abstract: High quality polymer free CO_2 foam possesses unique properties that make it an ideal fluid for fracturing unconventional shales. In this paper, the viscosity of polymer free fracturing foam and its empirical correlations at high pressure high temperature (HPHT) as a function of surfactant concentration, salinity, and shear rate are presented. Foams were generated using a widely-used surfactant, i.e., alpha olefin sulfonate (AOS) in the presence of brine and a stabilizer at HPHT. Pressurize foam rheometer was used to find out the viscosity of CO_2 foams at different surfactant concentration (0.25–1 wt %) and salinity (0.5–8 wt %) over a wide range of shear rate (10–500 s^{-1}) at 1500 psi and 80 °C. Experimental results concluded that foam apparent viscosity increases noticeably until the surfactant concentration of 0.5 wt %, whereas, the increment in salinity provided a continuous increase in foam apparent viscosity. Nonlinear regression was performed on experimental data and empirical correlations were developed. Power law model for foam viscosity was modified to accommodate for the effect of shear rate, surfactant concentration, and salinity. Power law indices (K and n) were found to be a strong function of surfactant concentration and salinity. The new correlations accurately predict the foam apparent viscosity under various stimulation scenarios and these can be used for fracture simulation modeling.

Keywords: CO_2 foam; foam apparent viscosity; viscosity correlation; salinity; surfactant concentration

1. Introduction

Unconventional reservoirs, such as shales, have garnered much attention due to their significant amount of stored reserves [1–4]. These huge reserves are unlocked by fracturing shales [5]. When the shales are fractured using conventional aqueous based polymer solutions, the plugging of nanopores takes place [6–11]. These conventional fracturing fluids need high amount of fresh water, increases the formation damage especially in the water sensitive zones and decreases the liquid recovery [9,11]. Gas fracking or pneumatic fracking is one of the alternative and highly beneficial methods for enhancing gas production from shales. Utilizing gas avoids various issues including water flowback, formation damage, clay swelling, and water requirements. In addition, the expansion of gas phase after treatment helps to recover the introduced liquid phase into the formation. CO_2 gas is more beneficial due to relatively high adsorption ability as compared to CH_4, which is a good aspect for releasing the adsorbed gas and underground carbon sequestration [5,9,12–17].

CO_2 injection alone is not suitable quite often because it has the limitation of low viscosity, limited possibility to operate at depth, and limited proppant carrying ability [10]. CO_2 foam, which is the

dispersion of CO_2 into a small amount of surfactant solution is considered as an ideal fracturing fluid for a variety of reasons, such as high viscosity, good thermal stability, good proppant carrying ability, especially in high temperature CO_2 environment, stable rheological performance as compared to polymers, reduction in polymer loading, elimination of the need for crosslinking gels and polymers, maximize cleanup of proppant packed, controls fracture, and apart from these, it has a lower amount of health hazardous chemical additives with less usage of fresh water [8,18]. It is highly desirable that the foam should have high stability and high viscosity for efficient job completion under various reservoir design and operating conditions.

Flow behavior of the foam is difficult to predict and the rheological characterization of foam is considered a complicated task [19]. In recent research on foam, it was stated that foam rheology has an important impact on foam hydraulic fracturing and the process efficiency depends on the non-Newtonian behavior of foam [20,21]. In order to describe the foam flow behavior, Power-law or Ostwald-de Waele model is one of the most commonly used models [7,20,22–27]. The mathematical form of power law is shown below in Equation (1).

$$\mu = K\gamma^{n-1} \tag{1}$$

where μ is the viscosity, γ is the shear rate, K is the flow consistency index, and n is the flow behavior index. The power-law fluids should yield a straight line on log-log scale with a negative slope.

Apparent viscosity of foam is dependent on the presence of chemical additives, salinity, foam quality, injection pressure, and reservoir temperature [7,20,21,28], and the controlled experiments are required to investigate the influence of each parameter.

The two important parameters i.e., surfactant concentration and salinity, strongly influence the foam apparent viscosity and are the main focus of this study. Selecting appropriate surfactant and its concentration for a stable foam generation under a specific set of conditions is a crucial task. Aronson et al. (1994) presented disjoining isotherms at two different surfactant concentrations and found high disjoining pressure at high surfactant concentration [29]. Higher disjoining pressure results in an increase in pressure gradient and resistance during the foam flow. Apaydin and Kovscek (2001) studied the effect of surfactant concentration and found that weak foam appears at low surfactant concentration and vice versa [30]. Gu and Mohanty (2015) studied the rheology of polymer free fracturing foam and considered two different concentrations (0.1 and 0.5 wt %) of anionic surfactant at high pressure high temperature (HPHT) [7]. They found highly viscous foam at a higher concentration of surfactant, which is attributed to the increase in total interfacial area of foam structure and it provides additional stability to foam lamella [7]. It is important for the foam film to be somewhat elastic in order to withstand deformation and the restoring force is provided by the Gibbs-Marangoni effect [31]. It has been reported that there is no strong and direct relationship available between foam stability and elasticity [31,32]. However, several researchers presented a positive relationship between foam stability and surface elasticity [33–37]. Increasing surfactant concentration increases the micelles network and this is able to affect surfactant packing arrangement on the lamella surface [34]. Gibbs-Marangoni effect dictates that there is maximum foaming performance at the intermediate range of surfactant concentration [34]. At very high concentration of surfactant, the foam stability decreases due to the decreases in surface elasticity, as indicated by slower counteraction toward the disturbing forces [34].

Surfactant micelles can be tuned with the packing parameter (P) of surfactant, i.e., $P = v/(a_o l_c)$, where v is volume of surfactant tail, l_c is the tail length, and a_o is the area of surfactant headgroup [38]. By the addition of electrolyte, the micelles of ionic surfactants that are in spherical shape are transformed to elongated spherocylinders (known as wormlike micelles), which consist of a cylindrical body with two hemispherical end caps. This screening of the electrostatic repulsive forces between the surfactant head decreases the effective area (a_o) [39,40]. The viscoelasticity is imparted by entanglement of wormlike micelles into a three dimensional network, similar to the behaviour of viscoelastic polymer solution [38]. Anionic surfactants may form wormlike micelles in the presence of electrolyte [41]. For the micelles of different surfactants such as sodium dodecyl sulfate (SDS), sodium lauryl ether

sulfate (SLES), and sodium/potassium oleate, the viscosity increases significantly upon increasing the packing parameter due to the addition of electrolyte [38]. Another study reported that the ability of surfactant to generate a viscous foam depends on the hydrophilic/lipohilic balance (HLB) of surfactant and HLB changes as the salt concentration varies [42]. Bulk foam viscosity of Decyl trimethylammonium bromide (DTAB) was found to decrease with the increase in salinity, whereas the Cetyl trimethylammonium bromide (CTAB) foam showed an increasing trend with the increase of salt concentration. Bulk foam of Mackam CB-35 (Rhodia surfactant) showed a decreasing trend in apparent viscosity until 3 wt % salinity, and after that a significant increase was observed [42].

It is concluded from the above literature that the foam behavior is non-Newtonian and that foam viscosity is strongly dependent on surfactant concentration and salinity. This study has quantified viscosity of CO_2 foam as a function of surfactant concentration, salinity, and shear rate. A fairly stable foam was generated utilizing commercial AOS in the presence of a foam stabilizer at HPHT, and a wide range of surfactant concentration (0.25–1 wt %), salinity (0.5–8 wt %), and shear rate (1–500/s) were considered. Based on experimental data, the empirical models for foam apparent viscosity as a function of surfactant concentration and salinity are presented.

2. Experimental Methodology

A widely used anionic $C_{14–16}$ Alpha Olefin Sulfonate (AOS, AkzoNobel, Chicago, IL, USA) was used as primary surfactant for foam generation. It was supplied with the percentage purity of 39%. TEGO Betaine C 60 was used as foam stabilizer. It was provided by Evonik Industries (Evonik Industries AG, Essen, Germany) with the percentage purity of 32.6%. The concentration of stabilizer was fixed to 0.5 wt % in this study. CO_2 gas with a purity of 99.98% was supplied from a 900 psi gas cylinder. All of the experiments were conducted at a temperature and pressure of 1500 psi and 80 °C. Different active concentrations (0.25–1 wt %) of surfactant solutions were prepared by mixing appropriate amount of surfactant stabilizer in brine. A wide range salinity (0.5–8 wt %) was considered in this study.

Foam rheology was studied using Pressurized Foam Rheometer model 8500 (shown in Figure 1) by Ametak Chandler Engineering (Chandler Engineering, IL, USA). The system comprises of several components, including a recirculation loop, sample accumulator, positive displacement (PD) pump, Coriolis mass flow controller, HPHT view cell, charged couple device (CCD) camera, backpressure regulator, and flow control valves for liquid and gas.

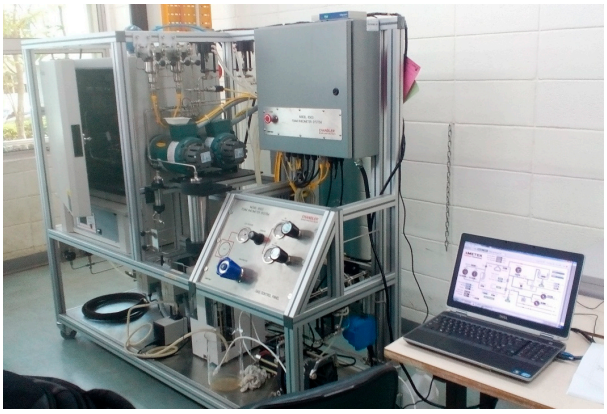

Figure 1. Pressurized foam rheometer model 8500.

A general system diagram of foam rheometer is shown in Figure 2. The system was designed specifically to measure the rheology of foam at high pressure and temperature over a wide range of shear rate. Foam was circulated in a small diameter steel pipe of circular shape, known as the recirculation loop or flow loop. The internal diameter and length of the test section was 0.775 cm

and 304.8 cm. Quizix pump was operated and the foaming solutions of different active components was transferred from the sample accumulator to the recirculation loop. The injection was continued until the loop pressure of 1500 psi was reached. Prior to the sample loading, it was ensured that the loop is free from any remnants. The oven temperature was set to 80 °C. A PD pump, attached to the recirculation loop, was operated at 500 s^{-1}, whereas, the speed of the foam generator was set to 50–100%. The needle valve attached to the flow loop was slowly opened and the 80% of liquid volume was slowly discharged into a graduated cylinder. During the process of liquid discharge, the testing pressure of 1500 psi was maintained in the loop. Gas booster was operated to reach high pressure of 1500 psi. In this way, the foam quality of 80% was achieved inside the recirculation loop. The circulation of the generated foam was continued until the foam density in the loop stabilized. The system software collected the data of differential pressure (ΔP) at different tested shear rate. Hagen-Poiseulle equation was then used to calculate the apparent viscosity of bulk foam and is represented as Equation (2) below [20,38,42,43].

$$\mu_{app} = \frac{D^2 \Delta P}{32LU} \quad (2)$$

where, D is the pipe diameter (cm), ΔP is the pressure drop across the test section (psi), L is the length of test section (cm), and U is the velocity (cm/s).

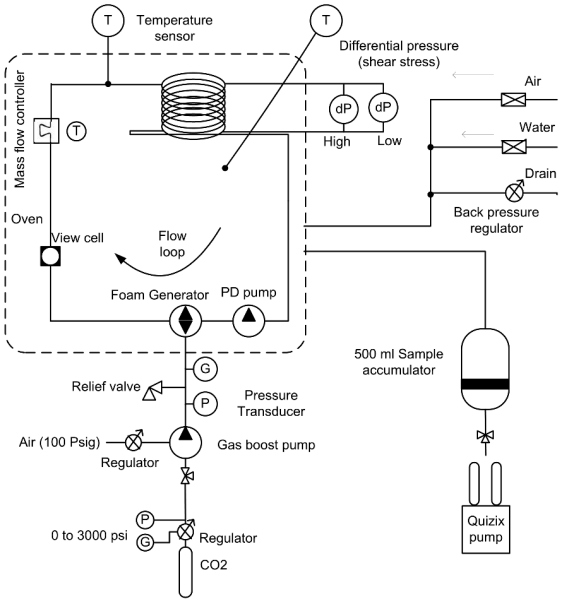

Figure 2. A system diagram of foam rheometer model 8500.

In this study, the experiments were not repeated to check the error during each test due to the time consuming and resource intensive nature of foam rheology study at high pressure and temperature condition. However, these experiments were conducted with high care using the procedure provided by manufacturer (Ametak Chandler Engineering). Previous studies have employed the flow loop rheometer for the rheological study of bulk foam [7,20,23,44–46].

3. Results and Discussion

3.1. Effect of Shear Rate

The effect of shear rate on the apparent viscosity of CO_2 foam is presented in Figure 3 and 7. The changes in the viscosity of foam was found to be the power law function of shear rate. All of the tested foams displayed shear thinning behavior within the entire tested range of shear rate (10 s^{-1} to 500 s^{-1}). This decrease in viscosity is due to Rayleigh-Taylor instability in shear flow, which results in

tensile deformation, stretching, and rupturing of foam bubble film [20,43]. Apparent viscosity of CO_2 was found to be changing with the change in surfactant concentration and salinity, and is discussed in detail in Sections 3.2 and 3.3.

Two data sets given in Table 1 were considered for the viscometric experiments and power law fitting was performed on the experimental data. The parametric estimates i.e., flow consistency index (K) and flow behavior index (n) were obtained by fitting power law (Equation (1)), as shown in Table 1. The coefficient of determination (R^2) value is given in Table 1. It is found that the R^2 values for all of the curve fittings were close to unity indicating good fit of the power law model.

Table 1. Power law parameter estimates for CO_2 foams.

	Surfactant Concentration (wt %)	Betaine Concentration (wt %)	Salinity (wt %)	Parameter Estimates		R^2
				K (mPa·s)	n (unitless)	
Set A	0.25	0.5	3	924.23	0.494	0.999
	0.5	0.5	3	2121	0.405	0.997
	1	0.5	3	2659.5	0.34	0.999
Set B	0.5	0.5	0.5	1080.2	0.529	0.996
	0.5	0.5	1.5	1591.2	0.459	0.999
	0.5	0.5	3	2121	0.405	0.999
	0.5	0.5	5	2344.4	0.41	0.999
	0.5	0.5	8	2683.2	0.433	0.98

3.2. Effect of Surfactant Concentration

The performance of CO_2 foam depends on the concentration of primary surfactant. In this study, the concentration of primary surfactant i.e., AOS was varied and its effect on the viscosity of CO_2 foam was studied. Three different AOS concentrations i.e., 0.25 wt %, 0.5 wt % and 1 wt % were tested in the presence of fixed amount of salinity and stabilizer at 80 °C and 1500 psi. Figure 3 presents the effect of surfactant concentration at fixed foam quality of 80%. From the figure, it can be noticed that the increase of surfactant concentration has shown a profound increase in foam apparent viscosity in the entire tested range of shear rate. The increase in foam apparent viscosity was found to be considerably high until 0.5 wt % and above, in which a slight decrease in foam viscosity was noticed. The decrease in viscosity above 0.5 wt % was found prominently at shear rate higher than 100 s^{-1}. With the increase of surfactant concentration, the network of micelles in foam lamella increases, causing an increase in disjoining pressure hence providing a high foam apparent viscosity [7,29,34]. On the other hand, at higher concentrations of 1 wt %, a slight decrease in foam viscosity was noticed. In this case, the tendency of micelle formation increases influencing the surfactant arrangement at the surface layer, which results in a faster liquid drainage to Plateau border, and hence reduces the surface elasticity [34]. From this set of experiments, the optimum concentration of AOS was found to be 0.5 wt %.

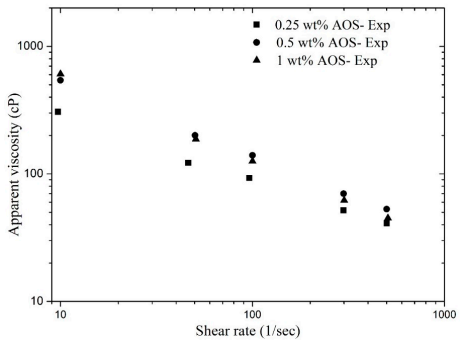

Figure 3. Effect of different alpha olefin sulfonate (AOS) concentration and shear rate on CO_2 foam apparent viscosity.

Considering all the parameters fixed (i.e., foam quality, temperature, pressure, NaCl, and Betaine concentration) and varying only the concentration of primary surfactant (AOS) in the foaming solution, the value of parameter K and n was found to be changing as shown in Table 1. For simplicity, a dimensionless concentration (C_D) has been introduced and it was defined as follows:

$$C_D = \frac{(C - C_{ref})}{C_{ref}} \tag{3}$$

where C is testing concentration and C_{ref} is reference concentration.

The reference concentration is taken as 0.25 wt %. The value of C_D for each tested surfactant concentration is listed in the following Table 2.

Table 2. AOS Concentrations and their respective dimensionless concentration.

Concentration (ppm)	Dimensionless Concentration, C_D (Unitless)
0.25	0
0.5	1
1	3

While studying K and n parameters individually, it was found that parameter k is a quadratic function of dimensionless concentration, as shown in Equation (4). Meanwhile, the parameter n is related to dimensionless concentration through a linear equation as shown in Equation (5). Figure 4 presents the matches between observed and predicted values and an acceptable trend was noticed. The proposed equations for K and n are given below.

$$K = g_1 {C_D}^2 + g_2 C_D + g_3 \tag{4}$$

$$n = h_1 C_D + h_2 \tag{5}$$

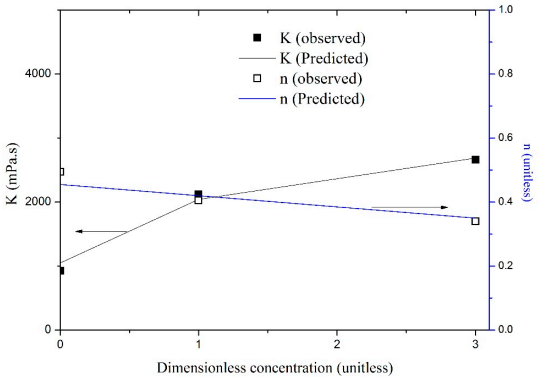

Figure 4. Effect of pressure on power-law parameters K and n on CO_2 Foam.

Substituting values of K and n in Equation (1) gives a new and modified form of power law model, which incorporates the effect of dimensionless concentration and shear rate, and is given by Equation (6).

$$\mu = (g_1 {C_D}^2 + g_2 C_D + g_3)\gamma^{(h_1 C_D + h_2 - 1)} \tag{6}$$

where g_1, g_2, g_3, h_1, and h_2 are the equation coefficients determined by performing non-linear regression on experimental data of foam viscosity using modified model (Equation (6)). The parameter estimates of this equation are available in Table 3. Viscometric data of foam was compared with the predicted viscosity values using Equation (6). R^2 and RMS values for this model was appeared to be 0.999 and 4.8,

respectively. This high value of R^2 and low magnitude of RMS indicated that Equation (6) has modeled the experimental data. In addition, Pearson's chi-square test was also conducted to test the goodness of fit of experimental data and predicted values using model Equation (6). The Pearson Chi-square value obtained from the test was 0.476 and the model was tested within the confidence interval of 95%. The *p* value was found to be 0.993, indicating a good fit of data. Figure 5 shows that the match between experimental and predicted data was quite good. This indicates that the developed model is able to predict foam apparent viscosity as a function of shear rate and surfactant concentration.

Table 3. Parameter estimates of viscosity correlation Equation (6) for CO_2 foam as a function of temperature and shear rate.

Parameter Estimates			
Parameter	**Estimate**	**Standard Error (%)**	**R^2**
g_1	−212.31	5.7	
g_2	1287.583	3.74	
g_3	1059.9	4.0	0.999
h_1	–0.05	7.0	
h_2	0.454	2.86	

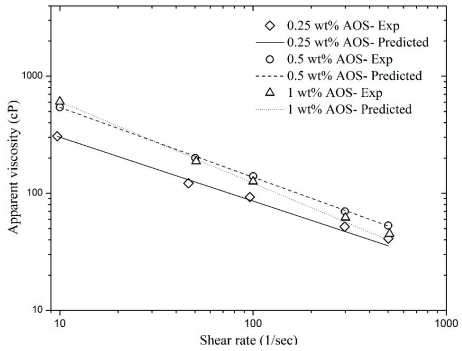

Figure 5. Matches between the experimental data and the predicted values (using Equation (6)) of CO_2 foam apparent viscosity as a function of shear rate and AOS concentration.

The model validation was also performed by utilizing the hidden data of experiments that were not utilized in the nonlinear regression analysis. The validation of Equation (6) is shown in Figure 6. It is clear from the figure that the matches between hidden experimental data and the predicted values using Equation (6) are very good. The maximum relative error was found to be 8.5%. This indicates that Equation (6) is an excellent predictor of foam apparent viscosity as a function of surfactant concentration and shear rate within the tested range.

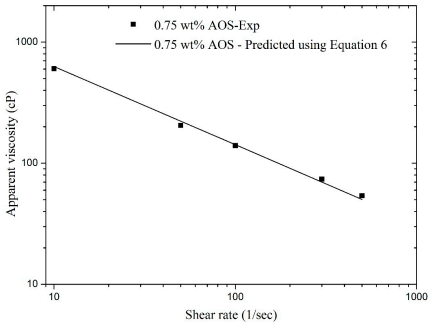

Figure 6. Validation of Equation (6).

3.3. Effect of Salinity

Five different NaCl concentration ranging from 0.5–8 wt % were tested while keeping all of the other parameters fixed and the effect of salinity on the foam apparent viscosity and shear rate was quantified. This series of experiments were conducted using fixed surfactant concentration i.e., 0.5 wt % AOS. The temperature and pressure for this series of experiments were fixed to 80 °C and 1500 psi. Figure 7 presents the effect of shear rate versus foam apparent viscosity by varying NaCl concentration. It can be observed that the increasing salinity has improved the foam apparent viscosity. A continuous increasing trend in foam apparent viscosity was noticed with the increase of salinity within the tested range of shear rate. This might be induced by the transformation of micellar structure through the favorable interactions between salt ions and oppositely changed surfactant head group [47,48]. However, the authors do not have any experimental evidence for this argument. The maximum foam viscosity was observed at the highest salinity (8 wt % NaCl).

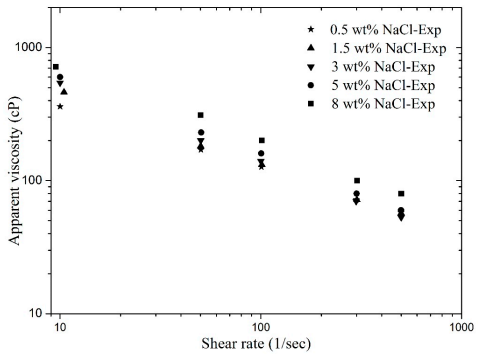

Figure 7. Effect of different salinity and shear rate on CO_2 foam apparent viscosity.

It is noticed that when varying the salinity of the foaming solution, the value of power law indices K and n for the foam also changes Both Power law parameters (K and n) were found to be a quadratic function of salinity, as shown in Equations (7) and (8). The matches between the observed and predicted values of K and n using Equations (7) and (8) are presented in Figure 8. It is clear from the figure that the matches between observed data and predicted values of K and n are considerably good. Hence, based on the results, the equations for K and n that account for the effect of salinity of the foaming solution are given by:

$$K = l_1 Salinity^2 + l_2 Salinity + l_3 \quad (7)$$

$$n = m_1 Salinity^2 + m_2 Salinity + m_3 \quad (8)$$

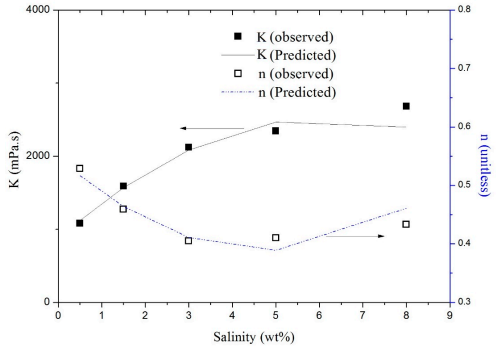

Figure 8. Effect of salinity on power-law parameters K and n on CO_2 foam.

Substituting equations of K and n in Equation (1) yield a modified version of power law that accounts the effect of salinity and shear rate, as shown in Equation (9).

$$\mu = (l_1 Salinity^2 + l_2 Salinity + l_3)\gamma^{(m_1 Salinity^2 + m_2 Salinity + m_3) - 1} \quad (9)$$

In Equation (9), l_1, l_2, l_3, m_1, m_2, and m_3 are parameter coefficients whose values were determined by performing nonlinear regression analysis on a straight line region of experimental data. The best fit parameters for Equation (9) are available in Table 4. The matches between experimental data and predicted values using Equation (9) is shown in Figure 9. R^2 and RMS values were appeared to be 0.998 and 5.26, respectively, indicating Equation (9) to be the good model for experimental data. In order to further validate the model, Pearson's chi-square test was also conducted to test the goodness of fit of model presented in Equation (9), on the experimental data. Chi-square value obtained was 4.523 and the model was analyzed within the confidence interval of 95%. The p value from this test was found to be 0.7178 indicating a good fit of model. This concludes that the prediction of apparent viscosity using the newly developed model is quite accurate.

Table 4. Parameter estimates of viscosity correlation Equation (9) for CO_2 foam as a function of temperature and shear rate.

Parameter Estimates			
Parameter	**Estimate**	**Standard Error (%)**	**R^2**
l_1	−43.273	6.8	0.998
l_2	538.338	5.57	
l_3	859.755	3.57	
m_1	0.007	7.28	
m_2	−0.067	5.62	
m_3	0.549	3.09	

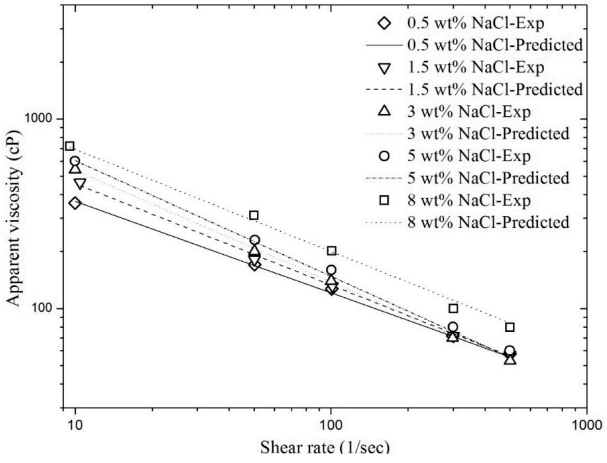

Figure 9. Matches between the experimental data and the predicted values (using Equation (9)) of CO_2 foam apparent viscosity as a function of shear rate and salinity.

The developed model (Equation (9)) for the effect of salinity and shear rate was also validated and shown in Figure 10. For the model validation, the experimental data that were not used in nonlinear regression were considered for the parametric estimation of Equation (9). A very good prediction was achieved and it is clear that the model is able to accurately predict the apparent viscosity of foam within the tested range of salinity. The maximum relative error was found to be 6.06%.

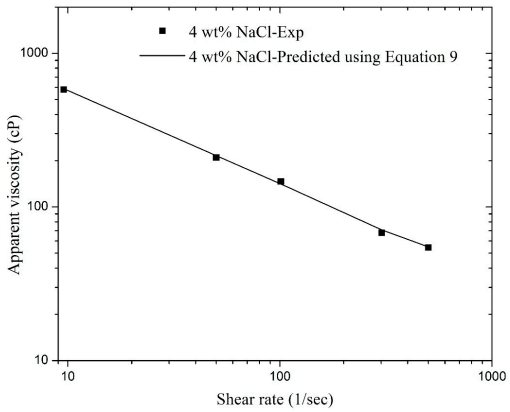

Figure 10. Validation of Equation (9).

4. Conclusions

Rheology of polymer free fracturing foam has been presented as a function of surfactant concentration and salinity at 1500 psi and 80 °C using a flow loop rheometer. Power law model for foam viscosity was modified and new empirical models have been presented that not only consider the effect of shear rate but also incorporate the impact of surfactant concentration and salinity.

Shear thinning behavior of foam was noticed at all of the tested surfactant concentrations and salinities. The optimum concentration of AOS was found to be 0.5 wt % and the concentration greater than 0.5 wt % did not increase the apparent viscosity. Whereas, the foam apparent viscosity has shown a direct relationship with the salinity of foaming solution. All of the tested foams have displayed power law behavior throughout the tested range of shear rate (10–500 s^{-1}).

Experimental data were utilized for nonlinear regression and modified power law models for foam apparent viscosity were generated. Power law indices (K and n) were found to be strongly dependent on surfactant concentration and salinity. The flow consistency index (K) was found to be a quadratic function of surfactant concentration, whereas, the flow consistency index (n) was fitted through a linear equation. Both of the K and n values were found to be the quadratic function of salinity. The new empirical correlations were found to be valid at all of the tested ranges of surfactant concentration (0.25–1 wt %), salinity (0.5 wt %–8 wt %), and shear rate (10–500 s^{-1}). These newly developed models were validated, and excellent matches were obtained between the experimental and predicted data. Additionally, these models can be incorporated into any fracturing simulator for the evaluation of foam fracturing efficiency.

Acknowledgments: The authors would like to thank Petroleum Engineering Department and Enhanced Oil Recovery Center at Universiti Teknologi PETRONAS for the funding (YUTP-0153AA-E70) and technical assistance in this work. The experimental part of this work was conducted in PETRONAS Research Sdn Bhd and authors highly acknowledge its laboratory setup. Akzonobel and Evonik are also deeply acknowledged for providing surfactant samples.

Author Contributions: All authors have contributed significantly to this work.

Conflicts of Interest: The authors declare no conflict of interest.

References

1. Harvey, T.; Gray, J. *The Unconventional Hydrocarbon Resources of Britain's Onshore Basins–Shale Gas*; The Department of Energy & Climate Change: London, UK, 2013.
2. Aguilera, R. Flow units: From conventional to tight-gas to shale-gas to tight-oil to shale-oil reservoirs. *SPE Reserv. Eval. Eng.* **2014**, *17*, 190–208. [CrossRef]
3. Cipolla, C.L.; Lolon, E.P.; Erdle, J.C.; Rubin, B. Reservoir modeling in shale-gas reservoirs. *SPE Reserv. Eval. Eng.* **2010**, *13*, 638–653. [CrossRef]

4. Mengal, S.A.; Wattenbarger, R.A. Accounting for Adsorbed Gas in Shale Gas Reservoirs. In Proceedings of the SPE Middle East Oil and Gas Show and Conference, Manama, Bahrain, 25–28 September 2011.
5. Lee, K.S.; Kim, T.H. *Integrative Understanding of Shale Gas Reservoirs*; Springer: Heidelberg, Germany, 2016.
6. Peles, J.; Wardlow, R.; Cox, G.; Haley, W.; Dusterhoft, R.; Walters, H.; Weaver, J. Maximizing well production with unique low molecular weight frac fluid. In Proceedings of the SPE Annual Technical Conference and Exhibition, San Antonio, TX, USA, 29 September–2 October 2002.
7. Gu, M.; Mohanty, K. Rheology of polymer-free foam fracturing fluids. *J. Pet. Sci. Eng.* **2015**, *134*, 87–96. [CrossRef]
8. Ribeiro, L.; Sharma, M. Fluid selection for energized fracture treatments. In Proceedings of the SPE Hydraulic Fracturing Technology Conference, The Woodlands, TX, USA, 4–6 February 2013.
9. Middleton, R.S.; Carey, J.W.; Currier, R.P.; Hyman, J.D.; Kang, Q.; Karra, S.; Jiménez-Martínez, J.; Porter, M.L.; Viswanathan, H.S. Shale gas and non-aqueous fracturing fluids: Opportunities and challenges for supercritical CO_2. *Appl. Energy* **2015**, *147*, 500–509. [CrossRef]
10. Barati, R.; Liang, J.T. A review of fracturing fluid systems used for hydraulic fracturing of oil and gas wells. *J. Appl. Polym. Sci.* **2014**, *131*, 40735. [CrossRef]
11. Makhanov, K.; Habibi, A.; Dehghanpour, H.; Kuru, E. Liquid uptake of gas shales: A workflow to estimate water loss during shut-in periods after fracturing operations. *J. Unconv. Oil Gas Resour.* **2014**, *7*, 22–32. [CrossRef]
12. Liu, F.; Ellett, K.; Xiao, Y.; Rupp, J.A. Assessing the feasibility of CO_2 storage in the new albany shale (devonian–mississippian) with potential enhanced gas recovery using reservoir simulation. *Int. J. Greenh. Gas Control* **2013**, *17*, 111–126. [CrossRef]
13. Busch, A.; Alles, S.; Gensterblum, Y.; Prinz, D.; Dewhurst, D.N.; Raven, M.D.; Stanjek, H.; Krooss, B.M. Carbon dioxide storage potential of shales. *Int. J. Greenh. Gas Control* **2008**, *2*, 297–308. [CrossRef]
14. Shi, J.-Q.; Durucan, S. Modelling of mixed-gas adsorption and diffusion in coalbed reservoirs. In Proceedings of the SPE Unconventional Reservoirs Conference, Keystone, CO, USA, 10–12 February 2008.
15. Edrisi, A.R.; Kam, S.I. A new foam rheology model for shale-gas foam fracturing applications. In Proceedings of the SPE Canadian Unconventional Resources Conference, Calgary, AB, Canada, 30 October–1 November 2012.
16. Heller, R. Laboratory measurements of matrix permeability and slippage enhanced permeability in gas shales. In Proceedings of the Unconventional Resources Technology Conference (URTEC), Denver, CO, USA, 12–14 August 2013.
17. Kang, S.M.; Fathi, E.; Ambrose, R.J.; Akkutlu, I.Y.; Sigal, R.F. Carbon dioxide storage capacity of organic-rich shales. *SPE J.* **2011**, *16*, 842–855. [CrossRef]
18. Luo, X.; Wang, S.; Wang, Z.; Jing, Z.; Lv, M. Experimental research on rheological properties and proppant transport performance of grf–CO_2 fracturing fluid. *J. Pet. Sci. Eng.* **2014**, *120*, 154–162. [CrossRef]
19. Gandossi, L. *An Overview of Hydraulic Fracturing and Other Formation Stimulation Technologies for Shale Gas Production*; Eur. Commisison Jt. Res. Cent. Tech. Reports; Publications Office of the European Union: Luxembourg, 2013.
20. Sun, X.; Liang, X.; Wang, S.; Lu, Y. Experimental study on the rheology of CO_2 viscoelastic surfactant foam fracturing fluid. *J. Pet. Sci. Eng.* **2014**, *119*, 104–111. [CrossRef]
21. Edrisi, A.; Kam, S.I. A new foam model in pipes for drilling and fracturing application. *SPE J.* **2014**, *19*, 576–585. [CrossRef]
22. Green, D.W.; Willhite, G.P. *Enhanced Oil Recovery*; Henry L. Doherty Memorial Fund of AIME, Society of Petroleum Engineers: Richardson, TX, USA, 1998.
23. Pramudita, R.A.; Ryoo, W.S. Viscosity measurements of CO_2-in-water foam with dodecyl polypropoxy sulfate surfactants for enhanced oil recovery application. *Korea-Aust. Rheol. J.* **2016**, *28*, 237–241. [CrossRef]
24. Batôt, G.; Fleury, M.; Nabzar, L. Study of CO_2 foam performance in a ccs context. In Proceedings of the 30th International Symposium of the Society of Core Analysts, Snowmass, CO, USA, 21–26 August 2016.
25. Sherif, T.; Ahmed, R.; Shah, S.; Amani, M. Rheological correlations for oil-based drilling foams. *J. Nat. Gas Sci. Eng.* **2016**, *35*, 1249–1260. [CrossRef]
26. Ostwald, W. Ueber die geschwindigkeitsfunktion der viskosität disperser systeme. I. *Kolloid-Zeitschrift* **1925**, *36*, 99–117. [CrossRef]

27. Martins, A.; Lourenco, A.; Sa, C.; Silva, V., Jr. Foam rheology characterization as a tool for predicting pressures while drilling offshore wells in ubd conditions. In Proceedings of the SPE/IADC Drilling Conference, Amsterdam, The Netherlands, 27 February–1 March 2001.
28. Ahmed, S.; Elraies, K.A.; Forooozesh, J.; Bt Mohd Shafian, S.R.; Hashmet, M.R.; Hsia, I.C.C.; Almansour, A. Experimental investigation of immiscible supercritical carbon dioxide foam rheology for improved oil recovery. *J. Earth Sci.* **2017**, *28*, 835–841. [CrossRef]
29. Aronson, A.; Bergeron, V.; Fagan, M.E.; Radke, C. The influence of disjoining pressure on foam stability and flow in porous media. *Colloids Surf. A Physicochem. Eng. Asp.* **1994**, *83*, 109–120. [CrossRef]
30. Apaydin, O.G.; Kovscek, A.R. Surfactant concentration and end effects on foam flow in porous media. *Transp. Porous Media* **2001**, *43*, 511–536. [CrossRef]
31. Schramm, L.L. *Emulsions, Foams, and Suspensions: Fundamentals and Applications*; John Wiley & Sons: Weinheim, Germany, 2006.
32. Georgieva, D.; Cagna, A.; Langevin, D. Link between surface elasticity and foam stability. *Soft Matter* **2009**, *5*, 2063–2071. [CrossRef]
33. Wei, P.; Pu, W.; Sun, L.; Wang, B. Research on nitrogen foam for enhancing oil recovery in harsh reservoirs. *J. Pet. Sci. Eng.* **2017**, *157*, 27–38. [CrossRef]
34. Tadros, T.F. *Applied Surfactants: Principles and Applications*; John Wiley & Sons: Weinheim, Germany, 2006.
35. Bergeron, V. Disjoining pressures and film stability of alkyltrimethylammonium bromide foam films. *Langmuir* **1997**, *13*, 3474–3482. [CrossRef]
36. Stubenrauch, C.; Miller, R. Stability of foam films and surface rheology: An oscillating bubble study at low frequencies. *J. Phys. Chem. B* **2004**, *108*, 6412–6421. [CrossRef] [PubMed]
37. Espert, A.; Klitzing, R.v.; Poulin, P.; Colin, A.; Zana, R.; Langevin, D. Behavior of soap films stabilized by a cationic dimeric surfactant. *Langmuir* **1998**, *14*, 4251–4260. [CrossRef]
38. Xue, Z.; Worthen, A.J.; Da, C.; Qajar, A.; Ketchum, I.R.; Alzobaidi, S.; Huh, C.; Prodanović, M.A.; Johnston, K.P. Ultradry carbon dioxide-in-water foams with viscoelastic aqueous phases. *Langmuir* **2015**, *32*, 28–37. [CrossRef] [PubMed]
39. Walker, L.M. Rheology and structure of worm-like micelles. *Curr. Opin. Colloid Interface Sci.* **2001**, *6*, 451–456. [CrossRef]
40. Feng, Y.; Chu, Z.; Dreiss, C. Smart wormlike micelles. *Chem. Soc. Rev.* **2013**, *42*, 7174–7203.
41. Parker, A.; Fieber, W. Viscoelasticity of anionic wormlike micelles: Effects of ionic strength and small hydrophobic molecules. *Soft Matter* **2013**, *9*, 1203–1213. [CrossRef]
42. Nguyen, Q.; Hirasaki, G.; Johnston, K. *Novel CO_2 Foam Concepts and Injection Schemes for Improving CO_2 Sweep Efficiency in Sandstone and Carbonate Hydrocarbon Formations*; University of Texas at Austin: Austin, TX, USA, 2015.
43. Li, C.; Huang, Y.; Sun, X.; Gao, R.; Zeng, F.B.; Tontiwachwuthikul, P.; Liang, Z. Rheological properties study of foam fracturing fluid using CO_2 and surfactant. *Chem. Eng. Sci.* **2017**, *170*, 720–730. [CrossRef]
44. Ahmed, S.; Elraies, K.A.; Hashmet, M.R.; Shaifan, B.M.; Rohaida, S.; Hsia, I.C.C.; Bahrim, R.Z.K. Experimental investigation and optimization of polymer enhanced CO_2 foam stability and apparent viscosity. In Proceedings of the SPE Annual Technical Symposium and Exhibition, Dhahran, Kingdom of Saudi Arabia, 24–27 April 2017; Society of Petroleum Engineers: Dhahran, Kingdom of Saudi Arabia, 2017.
45. Ahmed, S.; Elraies, K.A.; Tan, I.M.; Hashmet, M.R. Experimental investigation of associative polymer performance for CO_2 foam enhanced oil recovery. *J. Pet. Sci. Eng.* **2017**, *157*, 971–979. [CrossRef]
46. Bonilla, L.F.; Shah, S.N. Experimental investigation on the rheology of foams. In Proceedings of the SPE/CERI Gas Technology Symposium, Calgary, AB, Canada, 3–5 April 2000.
47. Xu, Q.; Nakajima, M.; Ichikawa, S.; Nakamura, N.; Roy, P.; Okadome, H.; Shiina, T. Effects of surfactant and electrolyte concentrations on bubble formation and stabilization. *J. Colloid Interface Sci.* **2009**, *332*, 208–214. [CrossRef] [PubMed]
48. Pandey, S.; Bagwe, R.P.; Shah, D.O. Effect of counterions on surface and foaming properties of dodecyl sulfate. *J. Colloid Interface Sci.* **2003**, *267*, 160–166. [CrossRef] [PubMed]